JOURNAL OF GEOPHYSICAL RESEARCH, VOL. 98, NO. C9, PAGES 16,501–16,507, SEPTEMBER 15, 1993

Three-Dimensional Langmuir Circulation Instability in a Stratified Layer

SIDNEY LEIBOVICH AND AMIT TANDON[1]

Department of Mechanical and Aerospace Engineering, Cornell University, Ithaca, New York

Some reports of Langmuir circulations describe windrows at systematic angles to the local wind direction. Other observers find windrows in close alignment to the wind direction, but with a systematic drift sideways to the wind. These effects probably result from more than one physical cause. Here it is shown, by an analysis of the linear stability of the surface layer, averaged to remove surface wave fluctuations, that persistent small windrow angles can result from weak stable density stratification. In these cases, the linearly most unstable modes are found to be weakly three dimensional for the range of parameters considered. Possible surface windrow patterns include rolls mostly parallel to the wind but of finite length, with branching and merging, as well as parallel rolls inclined to the wind and drifting laterally with respect to the wind direction. For unstratified flow, steady two-dimensional rolls are preferred.

INTRODUCTION

Streaks may be formed on the sea surface by a variety of causes, including convergences due to internal waves, possibly instability of the Ekman layer, Langmuir circulation, as well as other convective motions. The hallmark of Langmuir circulation is windrows approximately parallel to the wind direction, especially when the water column is unstratified or stably stratified. Most reports of streaks attributed to Langmuir circulations do not indicate any systematic bias in windrow direction relative to the wind. Nevertheless, there are observations (specifically, *Faller* [1964] and *Katz et al.* [1965]) that have revealed a systematic angular deviation in a system of parallel windrows.

In the more commonly reported cases, individual windrows nearly parallel to the wind terminate after a finite distance or split into two, or two windrows coalesce into one. This branching process appears to result, at least some of the time, from a secondary instability of the system of parallel rolls. This origin of the branching process is a nonlinear effect not requiring density variations and has been explored by *Thorpe* [1992], *Tandon* [1992], and A. Tandon and S. Leibovich (in preparation).

The problem treated in this paper is more appropriate as a model for experiments in a wind-wave tank than as a model for phenomena in the mixed layer, since it assumes a rigid no-slip bottom, and the effects of the Coriolis acceleration are ignored. Nevertheless, the analysis shows that a small stable density stratification can lead either to persistent (small) angles of parallel windrows to the wind direction, or to the branching and merging of windrows otherwise aligned with the wind. Both patterns are time-periodic in a stationary reference frame, but each pattern results from a travelling wave, and so is steady in a frame of reference moving either across the wind (former case) or with it (latter case). These are effects of buoyancy, and arise at the linear level in a stability analysis of the current and its wind-wave interaction in the Craik-Leibovich (CL) theory [*Craik and Leibovich*, 1976] of Langmuir circulation as formulated by *Leibovich* [1977*b*]. Which pattern is described by the linear analysis depends on the choice of linear eigenfunctions combined, and so depends on initial conditions. A more complete analysis of which form is physically realizable requires a nonlinear (secondary stability) analysis not done here.

The angular deviation of windrows observed by *Faller* [1964] averaged about 13° to the right of the wind, and *Katz et al.* [1965] report a similar figure (with a smaller data set). The tendency to lie to the right of wind suggests, as Faller emphasizes, that the deviation is due to Coriolis effects. This is plausible, since the surface current on which Langmuir circulation is imposed can exhibit Ekman spiralling. This effect is not included in the present analysis, which shows that the angular deviation possible from the linear stability analysis is maximum at an intermediate value of the stratification. The largest angle found for the range of stratification investigated here is 5.3°, but windrows have an equal likelihood of being on either side of the wind. Furthermore, the speed of lateral drift associated with the angular deviation increases with stratification.

As noted by *Leibovich* [1983], in two dimensions the CL theory of Langmuir circulations is mathematically analogous to more extensively studied double diffusive convection problems (with unit Prandtl number and with a possibly nonlinear temperature profile). This is no longer true for the CL theory in three dimensions. The equations controlling the stability problem are more complex, and the parameter space is enlarged. For example, given the form of the depth variation of the Stokes drift and assuming eddy coefficients for diffusivity of momentum and heat, the problem depends on four dimensionless parameters R, Re_*, S, and τ. Even when we restrict consideration to the molecular value of the (inverse) Prandtl number in water, τ $(= 0.14)$, we are able to examine only a small corner of the remaining three-dimensional parameter space. The parameter R is a relative measure (analogous to a Rayleigh number in thermal convection) of the destabilizing effect of the vortex force due to wave-current interaction [*Leibovich*, 1983]; Re_* is a Reynolds number based on the friction velocity, layer depth, and eddy viscosity; and S is a measure of the stabilization due to buoyancy relative to viscous effects.

If α is the phase angle made by disturbance modes as measured from the wind direction (so $\alpha = \tan^{-1} m/k$, where

[1]Now at Centre for Earth and Ocean Research, University of Victoria, Victoria, British Columbia, Canada.

Paper number 93JC01234.
0148-0227/93/93JC-01234$05.00

k is the component of the wavenumber vector in the direction of the wind, and m is the component at right angles to the wind), then the main results of the stability analysis are as follows: (1) for a given S and Re_*, the system is unstable when R is increased above a critical value, $R_c(S, Re_*)$; (2) the most unstable modes are three-dimensional ($\alpha \neq 0$) for all $S > 0$; (3) for a fixed S, $|\alpha|$ at critical conditions has a maximum at $Re_* \approx 6$; (4) the maximum value of the angle α is reached at an intermediate value in the range $0 \leq S \leq 980$ studied here, achieving a value of 5.30° at $S = 120$; (5) for large values of Re_*, R_c approaches an asymptote whose value is an increasing function of S, with mRe_*^2 approaching a constant, $C_1(S)$; (6) for small values of Re_*, R_c approaches the same asymptote with m/Re_*^2 approaching $C_2(S)$; and (7) marginally unstable modes are oscillatory, and the resulting motion appears as travelling waves.

In the final section, we construct "windrow patterns" by computing trajectories of particles on the free surface advected by a velocity field found from our linear stability analysis.

FORMULATION

We consider a layer of water with a mean free surface at the plane $z^* = 0$ and with a no-slip bottom at $z^* = -d$, and infinite in x^* and y^* directions. A uniform wind stress $\tau_w = \rho u_*^2$, taken to be in the direction of the x^* axis, is applied at the surface. The temperature is taken to be $T(0)$ at the top of the layer and $T(0) - \Delta T$ at the bottom. Following CL theory [see *Craik and Leibovich*, 1976; *Leibovich*, 1977*a*,*b*], the wind stress is assumed to result in dominant surface waves and a weaker mean current evolving on a slower time scale. We follow the averaging process of *Leibovich* [1977*b*] in which the averaged effect of surface waves appears as a Stokes drift $\mathbf{U_S}$. The averaged equations governing the flow in this layer [*Leibovich*, 1983] are given by

$$\frac{\partial \mathbf{u}^*}{\partial t^*} + \mathbf{u}^* \cdot \nabla^* \mathbf{u}^* - \mathbf{U_S}^* \times \nabla^* \times \mathbf{u}^* = -\nabla^* \Pi^* + \beta g \theta^* \mathbf{k} + \nu_T \nabla^{*2} \mathbf{u}^*, \quad (1)$$

$$\frac{\partial \theta^*}{\partial t^*} + (\mathbf{u}^* + \mathbf{U_S}^*) \cdot \nabla^* \theta^* + w^* T^{*'}(z) = \alpha_T \nabla^{*2} \theta^*, \quad (2)$$

$$\nabla^* \cdot \mathbf{u}^* = 0, \quad (3)$$

where $\mathbf{u}^* = [U^*(z) + u^*, v^*, w^*]$, $\mathbf{U_S}^*$ is the Stokes drift, ν_T is the eddy viscosity, α_T is the eddy heat diffusivity, $U^*(z)$ is the steady steady mean current, and θ^* is the deviation of temperature from the mean.

Equation (2) corrects the corresponding equation in *Leibovich* [1977*b*] to include the advection of temperature by the Stokes drift in the energy equation as in G. H. Knightly and D. Sather (Langmuir circulations when the Stokes drift has a cross-wind component, preprint).

The mean current and the Stokes drift are both taken to be in the wind direction and only z^*-dependent. A simple basic flow and temperature profile distribution can be

$$\begin{aligned} T^*(z) &= T(0) + \Delta T z^*/d, & (4) \\ U^*(z) &= u_*^2 z/\nu_T + U_0^* & (5) \end{aligned}$$

where ν_T is the eddy viscosity assumed constant throughout the layer. A constant stress is applied at the mean top surface, so we take the top boundary to be stress-free for the velocity perturbations. We choose the bottom wall to be a rigid no-slip surface. This is appropriate for laboratory experiments in wind-wave tanks, and for water of shallow and approximately uniform depth. With this boundary condition, it is consistent to take $U_0^* = u_*^2 d/\nu_T$.

The governing equations are made nondimensional by scaling the length scales by depth d, the mean current velocity and the Stokes drift by ν_T/d, and time by d^2/ν_T. The two-dimensional linear stability problem (with variables independent of the x direction) has been solved before by *Lele* [1985] and, under the assumption of a constant stress lower boundary, by *Leibovich et al.* [1989] (henceforth referred to as LLM). In two dimensions with a constant Stokes drift gradient the governing equations are analogus to equations governing the thermohaline convection problem, and these analogies have been explored in detail in previous studies [*Cox et al.*, 1992*a*,*b*; LLM]. Following LLM, we take the gradient of the Stokes drift to be specified according to

$$\frac{\partial U_s}{\partial z} = \frac{\partial U_s}{\partial z}(0) h(z).$$

For simplicity, the Stokes drift gradient is taken to be a constant, that is, $h(z) = 1$. Our experience has shown that unless the length scale over which $h(z)$ varies is small compared with d, the qualitative features of the resulting motions do not depend on the form of h. Hence we take the form of Stokes drift to be

$$\mathbf{U_S} = \left[\frac{R(1+z)}{Re_*^2}, 0, 0\right]$$

where

$$R = (Re_*^2 d^2/\nu_T) \frac{dU_s^*}{dz^*}(0),$$

$$Re_* = u_* d/\nu_T.$$

The nondimensionalization leads to two other parameters affecting the problem,

$$S = \beta g \Delta T d^3/\nu_T^2,$$

which represents the stabilizing effect of the temperature distribution, and

$$\tau = \kappa_T/\nu_T,$$

the inverse of the (turbulent) Prandtl number. The scaling used for the streamwise perturbation u is chosen to be $u_*^2 d/\nu_T$, to compare with the linear stability results in two dimensions by *Lele* [1985]. Thus, $(u^*, v^*, w^*) = \nu_T/d(Re_*^2 u, v, w)$.

Consider small perturbations of the basic state in the form (u, v, w) and θ, that is,

$$\mathbf{v} = [U(z) + u, v, w],$$

$$T = T(z) + \theta.$$

The equation of continuity is written as

$$Re_*^2 u_x + v_y + w_z = 0. \quad (6)$$

The linearized form of governing equations are used since the perturbations are considered to be small. We eliminate v and p by using the linearized z and x components of the curl of the vorticity and continuity equations. We arrive at the following non-dimensional equations for the velocity perturbations and temperature [cf. *Leibovich*, 1977*b*] .

$$\Delta[w_t + (U+U_s)w_x] - \Delta^2 w = \Delta_1[S\theta - Rh(z)u] + \left[w_x\left(2Re_*^2 + \frac{Rh(z)}{Re_*^2}\right)\right]_z, \quad (7)$$

$$\Delta[u_t + (U+U_s)u_x + w] + \frac{S}{Re_*^2}\theta_{xz} = \left[w_x\left(2 + \frac{Rh(z)}{Re_*^2}\right)\right]_x + \frac{R}{Re_*^2}[uh(z)]_z + \Delta^2 u, \quad (8)$$

$$\theta_t + (U+U_s)\theta_x + w = \tau\Delta\theta, \quad (9)$$

where

$$\Delta = \frac{\partial^2}{\partial x^2} + \frac{\partial^2}{\partial y^2} + \frac{\partial^2}{\partial z^2},$$
$$\Delta_1 = \frac{\partial^2}{\partial x^2} + \frac{\partial^2}{\partial y^2},$$

and the subscripts x, z, t denote differentiation.

Parameter Estimates

We estimate the likely ranges of parameters based on typical oceanic values. For example, we have examined data obtained during the Mixed Layer Dynamics Experiment (MILDEX). These data are part of the data analyzed and presented by *Weller and Price* [1988]. For a period in early November, 1983, during the experiment the mixed layer was about 40 m deep. The winds were fairly light, and on November 2, the temperature gradient in the mixed layer ranged up to almost 4×10^{-3} K m^{-1}. The winds increased after November 6, reducing the temperature gradient roughly by a factor of 4 on November 7. This leads to a Brunt-Väisälä frequency of $N = 3 \times 10^{-3}$ s^{-1} or less. We can rewrite the stabilizing parameter S as

$$S = \frac{\beta g \Delta T d^3}{\nu_T^2} = \left(\frac{NdRe_*}{u_*}\right)^2 = Ri_* Re_*^2,$$

where Ri_* is a Richardson number based on the friction velocity and layer depth. For the example discussed, with $u_* = 1$ cm s^{-1}, we can estimate $S = (12Re_*)^2$, or less. According to *Cox and Leibovich* [1993], various estimates put Re_* between 5 and about 50; *Tandon* [1992] argues that a two-layer structure may be more appropriate, and estimates that close to the surface where the dissipation rates are high, Re_* may be as low as 2, while at greater depths the dissipation rates are smaller and $Re_* \approx 50$. We vary Re_* in a larger range for the numerical calculations in this paper, from $Re_* \approx 1$ up to $Re_* = 100$ for some runs. With $Re_* = 2$, we get $S = 576$ (or less). Note that for laboratory experiments, we expect significantly smaller values of S. We do the stability calculations at $S = 0, 10, 120$ and 980, respectively in this study, with $\tau = 1/6.7$ held constant, corresponding to the molecular Prandtl number for water. For these parameters, the corresponding values of the critical wavenumbers along and across the wind direction and the corresponding critical destabilizing Rayleigh number R, are then found.

Boundary Conditions

The system (7) and (8) is fourth order in w and u. We thus need four boundary conditions for u and w each, at both boundaries in z. Higher-order boundary conditions are derived by using the boundary conditions on v, the y component of velocity. Since the wind stress at the top surface is assumed constant, the perturbation velocity components carry no stress, that is,

$$u_z = 0, \quad (10)$$
$$v_z = 0, \quad (11)$$
$$w = 0. \quad (12)$$

Differentiating the equation of continuity (6) with respect to z, at $z = 0$ and using (10) and (11), we get

$$w_{zz} = 0. \quad (13)$$

We use the linearized y component of the vorticity equation to derive higher-order boundary conditions for u. This equation can be written as

$$\frac{\partial}{\partial t}(Re_*^2 u_z - w_x) + (U+U_s)\frac{\partial}{\partial x}(Re_*^2 u_z - w_x) - Re_*^2 v_y = -S\theta_x + \Delta(Re_*^2 u_z - w_x). \quad (14)$$

Recognizing that at the top boundary, $u_{zt} = w_{xt} = u_{zx} = w_{xx} = 0$, and using the continuity equation (6), we get

$$Re_*^2(Re_*^2 u_x + w_z) = -S\theta_x + \Delta(Re_*^2 u_z - w_x).$$

Again, at $z = 0$, $w_{xxx} = w_{xyy} = 0$ from (12), and $w_{xzz} = (w_{zz})_x = (-v_{yz} - Re_*^2 u_{xz})_x = 0$ from (6), (10), and (11). Similarly, $\Delta u_z = u_{zxx} + u_{zyy} + u_{zzz} = u_{zzz}$ at $z = 0$. Thus the boundary condition at the top boundary is

$$Re_*^4 u_x + Re_*^2 w_z = Re_*^2 u_{zzz} - S\theta_x. \quad (15)$$

In the stability analysis, (10), (12), (13), and (15) are used as boundary conditions at $z = 0$.

Various temperature boundary conditions may be appropriate: we set

$$\theta = 0 \qquad \text{at} \qquad z = 0, -1.$$

Since v has been eliminated, the no-slip conditions at the lower boundary are

$$u = 0, \quad (16)$$
$$w = 0, \quad (17)$$
$$w_z = 0, \quad (18)$$

where we have used (6) to get the last boundary condition. In addition, we derive a higher-order boundary condition from the y component of the vorticity equation (14). Recognizing that $w_{xt} = w_{xx} = v_y = w_{xxx} = w_{xyy} = 0$ at the bottom wall, $z = -1$, equation (14) reduces to

$$Re_*^2[u_{tz} + (U+U_s)u_{xz}] = Re_*^2(\Delta u_z) - w_{xzz} - S\theta_x. \quad (19)$$

Assuming normal mode form for the perturbations,

$$(u, v, w, \theta) = Re\{[u(z), v(z), w(z), \theta(z)]\exp[i(mx + ky) + \sigma t]\} \quad (20)$$

results in a tenth-order eigenvalue problem. The equations for u and w are each fourth order in z, and θ is second order, with 10 boundary conditions. The eigenvalue σ depends on the following parameters:

$$\sigma = \sigma(m, k; R, S, Re_*, \tau).$$

Here, m is the wavenumber of the disturbance in the wind direction and k is the wavenumber of the disturbance in the cross-wind direction. This perturbation is at an angle $\tan^{-1}(m/k)$ to the wind.

The equations are solved by using a spectral tau-collocation method employing Chebyshev polynomials, and the eigenvalues obtained by solving the corresponding matrix eigenproblem. The eigenvalue problem is solved using the double-precision complex version of the QZ algorithm [cf. *Golub and VanLoan*, 1991] . We consider the resolution to be sufficient when the eigenvalues are resolved to four significant places. The corresponding maximum change in the eigenfunction $\|X_{N2} - X_{N1}\|/\|X_{\max}\| \approx 10^{-4}$ for the most unstable eigenfunction.

Independent checks were made to test the accuracy of some eigenvalues. Analogies with double diffusive systems with different boundary conditions can be made when the perturbations are taken to be two-dimensional. We have checked the eigenvalues against the analytical expressions available for the linear double diffusive systems [*Huppert and Moore*, 1976]. From equation (2.6*b*) of their paper, $R_c = 898.3088$ and $\sigma_i = \pm 1.46696$, corresponding to the parameters $\tau = 0.15$, $k = \pi/\sqrt{2}$ and $S = 50$ in our formulation, with appropriate boundary conditions. Our linear stability code gives us $R_c = 898.3088$ and $\sigma_i = \pm 1.46697$. In the absence of the Stokes drift and stratification terms, the system of equations reduces to those governing unstratified Couette flow. For unstratified Couette flow, we compare our results with those of *Gallagher and Mercer* [1962]. From their paper, for $\alpha = 4$, $R = 1$, $\lambda_1' = 1.70 + 0.0i$ which corresponds to $\sigma = -80.7783 - 4.0i$, and from the spectral code with $N = 24$, we get $\sigma = -80.7298 - 4.0i$. The eigenvalue checks were done against *Lele* [1985] for the cases where perturbations are independent of x direction at different stratification (and Re_*) values. The eigenvalues for this case are independent of Re_*, as expected. For a linear Stokes drift gradient ($\lambda = 0$), at $S = 0$, $\tau = 0.15$ yields $R_c = 669.0, k_c = 2.09$ by the linear stability code which agrees with *Lele* [1985]. Some eigenvalues for three-dimensional modes were also checked against a shooting method using Newton's technique and numerical integrations using adaptively controlled step sizes [*Press et al.*, 1986]. For example, when $m = 0.2$, $k = 2.07$, $S = 20.0$, $Re_* = 10.0$, and $R = 760.0$, the spectral linear code gives $\sigma = -0.3461105 - 14.13044i$, while the shooting method gives $\sigma = -0.3461527 - 14.13035i$. The eigenvalues are also checked against mixed boundary conditions, as in *Cox and Leibovich* [1993]. For example, at mixed boundary condition parameters $\alpha_t = 0.06$, $\alpha_b = 0.4$, and $S = 0$, the critical values are $k_c = 1.2$, and $R_c = 211.701$, which checks with the linear stability results of S.M. Cox (private communication, 1991).

RESULTS

We search in parameter space for most unstable modes. The problem has the following symmetries:

$$\sigma(m, k; R, S, Re_*) = \sigma(m, -k; R, S, Re_*), \tag{21}$$

$$\sigma(m, k; R, S, Re_*) = \overline{\sigma}(-m, k; R, S, Re_*). \tag{22}$$

In the absence of stratification ($S = 0$), the energy equation decouples from the velocity equations and an eighth-order eigensystem of ODEs is solved. For these cases it is found that the critical neutral disturbance (one that corresponds to the highest growth rate with the least destabilizing Rayleigh number) is one with $m = 0$. This implies that two-dimensional disturbances render the system most unstable, as suggested by the energy stability analysis of *Leibovich and Paolucci* [1980]. For this case, the critical y wavenumber $k_c = 2.09$, $\sigma_i = 0$, and corresponding destabilizing Rayleigh number $R_c = 669.0$, independent of the Reynolds number. For a weak three-dimensional mode at $S = 0$, say, $m = 0.02$ and $Re_{*c} = 5.1$, $R_c = 669.27$ and $\sigma_i = -0.672$. At $Re_* = 1.0$, for $m = 0.02$ at $R = 669.0$, the growth rate $\sigma_r = -0.29$, and $\sigma_i = -8.710$. So, two-dimensional disturbances are most unstable for unstratified water.

For stratified flow, three-dimensional effects become important and most unstable modes correspond to ones with $m \neq 0.0$. The ratio of m to k still remains quite small, that is, length of critical rolls in wind direction is much longer than their width in cross-stream direction. In their energy stability analysis for an infinite depth layer, *Leibovich and Paolucci* [1980] concluded that the system is most unstable to two-dimensional disturbances, though they did not rule out the possibility of three-dimensional disturbances in a narrow band about $m = 0.0$ with a smaller region of global stability than at $m = 0.0$.

To confirm that three-dimensional disturbances are important at all nonzero values of S, we find the critical destabilizing Rayleigh numbers for a three-dimensional mode and compare it with the two-dimensional values of the critical Rayleigh number. This is done at $m = 0.02$ while S is varied from 10 to 200. The results appear in Table 1. The critical Rayleigh number R_c with increasing S for $m = 0.02$ is smaller than for $m = 0.0$, so three-dimensional disturbances are important. In Table 1, $\overline{Re}^2_{*c} \approx R_c/\underline{Re}^2_{*c}$, and $\underline{\sigma_i} \approx \overline{\sigma_i}$ since the dominant term in the eigenvalue problem for these parameters is $Re_*^2 + R/Re_*^2$. Another test run is done at constant stratification $S = 120.0$ and $R = 913.73$ for different values of Re_*. Then, $\sigma = \sigma(m_c, k_c, Re_{*c})$. The results appear in Table 2.

As Re_* is increased with R and S fixed, the growth rate decreases for an intermediate range in Re_*. R_c approaches the same asymptotic value $\underline{R_c}$ for $Re_* \gg 1$ and $Re_* \ll 1$ depending on S but independent of Re_*. For $Re_* \gg 1$, $m\,Re_*^2 \rightarrow$ const $= C_1$ for the most unstable mode; and for $Re_* \ll 1$, $m_c/Re_{*c}^2 \rightarrow$ const $= C_2$. Both asymptotic behaviors are clear from Tables 3 and 4.

To determine at what stratification S three-dimensional effects become important, and to determine how their characteristics vary with Re_* for a given stratification, we adopt the following strategy. Fix the stratification at a constant value S, and vary the Reynolds number from small to large

TABLE 1. Critical y Wavenumber, Critical Reynolds Number, Critical Rayleigh Number and Imaginary Part of the Eigenvalue for Various Stratification Values at $m = 0.02$

S	k_c	$\underline{Re}^2_{*c}$	$\overline{Re}^2_{*c}$	R_c	$\underline{\sigma_i}$	$\overline{\sigma_i}$
10	2.06	3.93	179	705.5	−2.45	−2.44
20	2.04	2.10	352	734.5	−4.75	−4.78
40	2.00	1.64	478	780.4	−6.58	−6.61
80	1.96	1.50	571	853.2	−8.12	−8.15
200	1.93	1.61	633	1016.7	−9.79	−9.81

For comparison, a restriction to two-dimensional modes ($m = 0$) at $S = 10$ yields $R_c \approx 745$ and at $S = 200$ yields $R_c \approx 1200$. $\underline{Re}^2_{*c}$ and $\overline{Re}^2_{*c}$ correspond to the lower and higher values of Re_* at which $m = 0.02$ mode is most unstable. $\overline{Re}^2_{*c} \approx R_c/\underline{Re}^2_{*c}$, and $\underline{\sigma_i} \approx \overline{\sigma_i}$ since the dominant term in the eigenvalue problem for these parameters is $Re_*^2 + R/Re_*^2$.

TABLE 2. Wavenumbers, Growth Rate and Imaginary Part of the Eigenvalue for the Most Unstable Modes at $S = 120$, $R = 913.73$ with Increasing Reynolds Number

Re_*^2	m_c	k_c	σ_r	σ_i
0.01	13.3×10^{-5}	1.94	0.0	−8.90
1	13.3×10^{-3}	1.94	0.0	−8.90
5	64.0×10^{-3}	1.94	-5.97×10^{-3}	−8.82
10	0.115	1.94	−0.02	−8.60
100	0.107	1.94	−0.0176	−8.61
500	0.024	1.94	0.0	−8.83
10^3	1.22×10^{-2}	1.94	0.0	−8.94

values and find (m_c, k_c, R_c) for each Re_*. For each of these runs, we can also determine the maximum deviation of the roll axis from the axis of the wind direction, defined as $\alpha = \tan^{-1}(m_c/k_c)$, in the process. The results for these calculations are presented in Tables 3, 4, and 5 corresponding to $S = 10$, 120, and 980, respectively. The tables show the variation against Re_*^2. This is the right scaling from the equations, and it also serves to enlarge the region of interest in Re_* where three-dimensional modes occur.

Some trends can be noted from Figure 1, which shows the maximum deviation of rolls from the wind direction for different values of stratification. At high and low Reynolds number the rolls are nearly aligned with the wind. There is an intermediate Reynolds number at about $Re_* = 6$ at which the roll angle α is a maximum. Figure 2 shows the corresponding values of $R_c - \underline{R_c}$. As stratification increases, the maximum angular deviation of roll axis from the wind direction increases to a maximum of 5.3° near $S = 120$ and decreases as the stratification is increased further. We can interpret the m_c/k_c ratio in two ways. One possible configuration is to imagine two-dimensional infinite rolls at an angle to the wind. This angle in our model depends on the stratification S and the Reynolds number Re_*. So, at marginally unstable values of R, one may, for example, observe rolls at an angle to the wind direction. This linear stability analysis cannot predict whether the left or right rolls would be stable, and one needs to include nonlinearity to investigate these effects. Another possible combination is to combine a left and a right mode to see two-dimensional rolls modulated in the direction of the wind. From Tables 3, 4, and 5 we see that the k_c variation is small, that is, critical roll width in the cross-wind direction is approximately the same. In this case one could interpret the m_c/k_c ratio to be a measure of the inverse of the windward roll length. Therefore at $S = 10$, the minimum roll length-to-width ratio is about 55.2; 10.77 at $S = 120$; and at $S = 980$ it is 12.97. An intermediate case for different amplitudes of left and right modes would show us both modulation in the x direction and rolls being at an

TABLE 3. Maximum Roll-Deviation From the Wind Axis at $S = 10$, With Varied Reynolds Number

Re_*^2	m_c	k_c	R_c	σ_i	α, deg.
0.1	5.2×10^{-4}	2.06	705.4	−2.45	0.014
1	5.2×10^{-3}	2.06	705.4	−2.45	0.14
10	3.5×10^{-2}	2.05	705.6	−1.88	1.00
30	3.5×10^{-2}	2.05	705.8	−1.24	1.00
40	3.60×10^{-2}	2.05	705.8	−1.39	1.01
50	3.71×10^{-2}	2.05	705.7	−1.63	1.04*
60	3.7×10^{-2}	2.05	705.7	−1.77	1.03
75	3.5×10^{-2}	2.05	705.6	−1.95	0.98
100	3.0×10^{-2}	2.05	705.5	−2.15	0.84
500	7.2×10^{-3}	2.06	705.4	−2.41	0.20
10^3	3.70×10^{-3}	2.06	705.4	−2.47	0.10
10^4	3.66×10^{-4}	2.06	705.4	−2.44	0.01

Also enlisted are the critical wavenumbers, Rayleigh number, and imaginary part of the eigenvalue.
* The maximum deviation is 1.04° at $Re_*^2 = 50$.

TABLE 4. Maximum Roll-Deviation From the Wind Axis at $S = 120$, With Varied Reynolds Number

Re_*^2	m_c	k_c	R_c	σ_i	α, deg.
1	13.3×10^{-3}	1.94	913.7	−8.90	0.39
10	0.115	1.94	917.0	−8.62	3.39
20	0.168	1.95	921.2	−8.26	4.92
25	0.178	1.95	922.4	−8.19	5.21
30	0.181	1.95	922.4	−8.20	5.30*
35	0.179	1.95	922.3	−8.18	5.24
40	0.175	1.95	921.8	−9.21	5.13
50	0.163	1.94	920.7	−8.28	4.80
10^2	0.108	1.94	916.6	−8.68	3.19
10^3	1.22×10^{-2}	1.94	913.7	−8.94	0.36
10^4	1.2×10^{-3}	1.94	913.7	−8.94	0.036

Also enlisted are the critical wavenumbers, Rayleigh number, and imaginary part of the eigenvalue.
* The maximum deviation is 5.30° at $Re_*^2 = 30$.

TABLE 5. Maximum Roll-Deviation From the Wind Axis at $S = 980$, With Varied Reynolds Number

Re_*^2	m_c	k_c	R_c	σ_i	α, deg.
1	8.9×10^{-3}	2.13	1764.1	−15.83	0.24
10	8.2×10^{-2}	2.14	1766.7	−15.64	2.19
20	0.14	2.16	1771.7	−15.66	3.71
30	0.16	2.18	1774.8	−15.19	4.20
35	0.166	2.18	1775.6	−15.17	4.35
40	0.168	2.18	1776.0	−15.24	4.41*
50	0.165	2.18	1775.8	−15.35	4.33
60	0.16	2.17	1774.8	−15.19	4.22
70	0.15	2.17	1773.7	−15.16	3.95
80	0.14	2.17	1772.6	−14.55	3.69
100	0.13	2.15	1770.6	−15.68	3.46
500	0.031	2.13	1764.4	−15.78	0.83
10^3	1.57×10^{-2}	2.13	1764.2	−15.84	0.42

The table also enlists the critical wavenumbers, Rayleigh number, and imaginary part of the eigenvalue.
* The maximum deviation is 4.41° at $Re_*^2 = 40$.

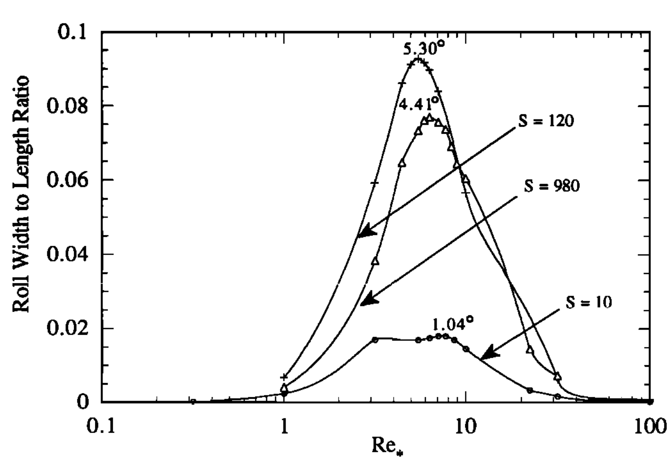

Fig. 1. Deviation of rolls from the wind direction. The maximum deviation is 1.04°, 5.30°, and 4.41° for $S = 10$, 120, and 980, respectively. An alternate interpretation is roll width-to-length ratios for various stratification values, characterizing three dimensionality of the most unstable mode.

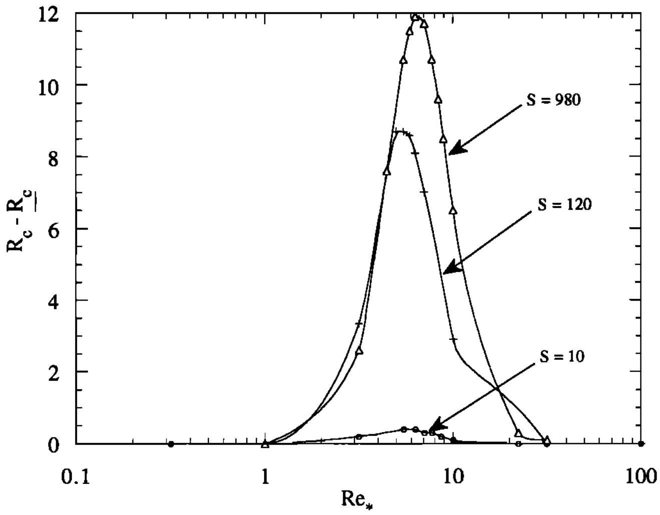

Fig. 2. The variation in critical value of the destabilizing Rayleigh number from its asymptotic value $R_c - \underline{R_c}$ with Re_* at $S = 10$, 120, and 980.

angle to the wind. The inclusion of nonlinear effects would shed some light on which of these states would actually be observed.

The imaginary part of the eigenvalue is nonzero, which indicates that most unstable modes are also time-dependent. For a 0.2-m layer, with $Re_* = 15$, $u_* = 1$ cm s^{-1}, the dimensional time periods are of the order of 13.1, 3.5, and 2.0 min at $S = 10$, 120, and 980, respectively. For a mixed layer with a depth of 40 m and the same value of Re_*, the time periods are increased by a factor of 200.

Discussion and Conclusions

Stratification causes the most unstable Langmuir circulation modes to be three-dimensional. For moderate values of stratification and physically reasonable values of Re_*, the maximum roll angle is small. For $Re_* > 15$, at $S = 120$ the maximum roll-deviation is less than 4°. For lower Re_* the maximum deviation is about 5.3°, and the maximum deviation appears at $Re_* \approx 6$.

We have calculated particular examples of surface windrow patterns based on our linear stability analysis to illustrate this effect. Windrows are formed by tracking 10,000 particles on the surface of the layer for $S = 120, R = 922.4$, and $Re_*^2 = 30$, subject to the marginally stable velocity field obtained from the linear stability analysis. The normalization of the linear perturbation is arbitrary, and the choice made for the figures sets the maximum surface windward velocity perturbation to be 7.6% of the undisturbed surface speed. The particles are passive tracers moving with this velocity field. The required data are given in Table 4. The numerical integrations are performed by using a Bulirsch-Stoer method [*Press et al.*, 1986] for the particle positions. We present two cases: a mode forming parallel rolls at an angle to the wind, obtained by taking a single unstable wavenumber $((m, k) = (0.181, 1.95))$ and a linear combination of the same mode but with both $m = \pm 0.181$ with equal amplitudes. The degree of organization for left and right amplitude windrows is time-dependent and windrow patterns rearrange themselves in time. Figure 3 shows the left mode for $R = 922.4$ and $Re_*^2 = 30$ at a streamwise wavelength-to-depth ratio of 34.7 and spanwise wavelength-to-depth ratio of 3.2, after five time periods of the linear mode. The streamwise and spanwise scales in this figure are scaled by the depth. The corresponding pattern for a single wavenumber roll with $m = -0.181$ is a mirror image of the pattern at $m = 0.181$. The linear combination of modes gives rise to a steady windrow pattern convected in the streamwise direction. This pattern is modulated in the streamwise direction as shown in Figure 4.

The pattern in Figure 3 is periodic in time with (angular) frequency $\omega = -8.20\nu_T/d^2$. Writing $\nu_T = u_* d/Re_*$, $|\omega| = 8.20(u_*/d)/Re_*$. The pattern would appear to be drifting from the top to the bottom of the page with a phase speed $c_1 = |\omega| d/m$, or $c_1 = 45.3u_*/Re_*$. For the example, $Re_* = \sqrt{30} = 5.5$, and so $c_1 = 8.3u_*$. For $u_* = 1$ cm s^{-1}, this gives a drift speed of about 8 cm s^{-1}.

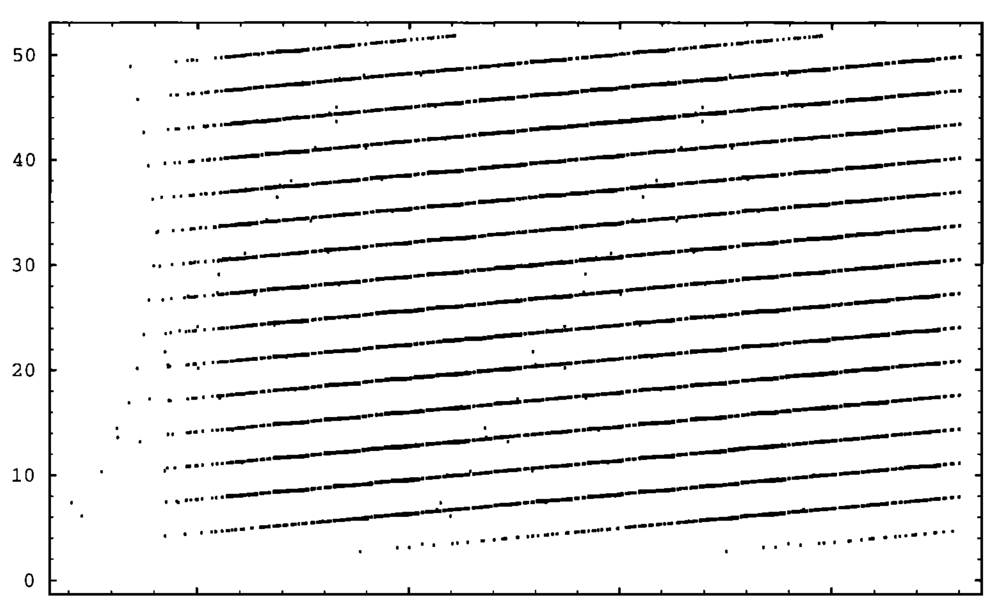

Fig. 3. Windrow pattern for the left mode at $m = 0.181$, $k = 1.95$, $Re_*^2 = 30$, and $R = 922.4$, at the end of five time periods. The initial field is an equally spaced field of 10,000 particles covering two wavelengths in the streamwise direction. The windrows are at an angle $\alpha = 5.3°$ to the wind direction.

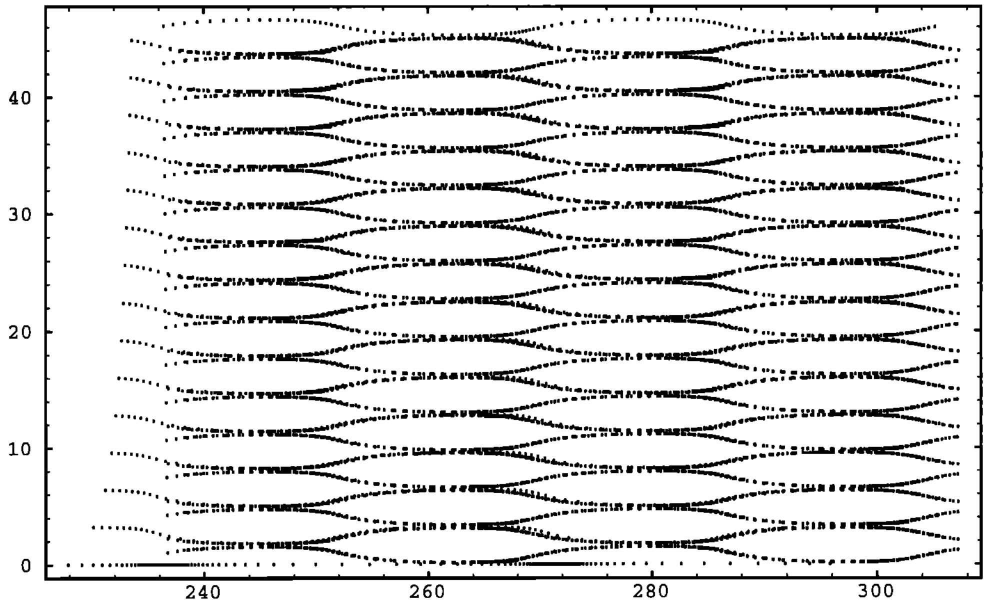

Fig. 4. Same windrow pattern as in Figure 3, with equal amplitudes of left and right modes.

The pattern in Figure 4 would appear to drift in the wind direction (to the right of the figure), with a phase speed $c_2 = |\omega| d/k = c_1 m/k$, or $c_2 \approx .8$ cm s^{-1}. Notice that the ratio of windward wavelength to crosswind wavelength in this figure is 10.77, so that the length-to-spacing ratio of the modulated rolls has this value for this particular example.

Acknowledgments. This work was supported by NSF OCE-90-17882 and ONR N00014-92-J-1547. We thank A. Ganapathian and R. A. Weller for supplying us the data obtained during MILDEX and R. Rutka for assistance in formatting this paper.

REFERENCES

Cox, S. M., and S. Leibovich, Langmuir circulations in a surface layer bounded by a strong thermocline, *J. Phys. Oceanogr.*, *23*, 1330–1345, 1993.

Cox, S. M., S. Leibovich, I. M. Moroz, and A. Tandon, Nonlinear dynamics in Langmuir circulations with O(2) symmetry, *J. Fluid Mech.*, *241*, 669–704, 1992a.

Cox, S. M., S. Leibovich, I. M. Moroz, and A. Tandon, Hopf bifurcations with O(2) symmetry in Langmuir circulations, *Physica D.*, *59*, 226–254, 1992b.

Craik, A. D. D., and S. Leibovich, A rational model for Langmuir circulations, *J. Fluid Mech.*, *73*, 401–426, 1976.

Faller, A. J., The angle of windrows in the ocean, *Tellus*, *16*, 363–370, 1964.

Gallagher, A. P., and M. A. Mercer, Small disturbances in plane Couette flow, *J. Fluid Mech.*, *13*, 91–100, 1962.

Golub, G. H., and C. F. VanLoan, *Matrix Computations*, Johns Hopkins University Press, Baltimore, Md., 1991.

Huppert, H. E., and D. R. Moore, Nonlinear double-diffusive convection, *J. Fluid Mech.*, *78*, 821–852, 1976.

Katz, B., R. Gerard, and M. Costin, Responses of dye tracers to sea surface conditions, *J. Geophys. Res.*, *70*, 5505–5513, 1965.

Leibovich, S., On the evolution of the system of wind drift currents and Langmuir circulations in the ocean. Part 1. Theory and averaged current, *J. Fluid Mech.*, *79*, 715–743, 1977a.

Leibovich, S., Convective instability of stably stratified water in the ocean, *J. Fluid Mech.*, *82*, 561–581, 1977b.

Leibovich, S., The form and dynamics of Langmuir circulations, *Annu. Rev. Fluid Mech.*, *15*, 391–427, 1983.

Leibovich, S., and S. Paolucci, Energy stability of the Eulerian-mean motion in the upper ocean to three-dimensional perturbations, *Phys. Fluids*, *23*, 1286–1290, 1980.

Leibovich, S., S. K. Lele, and I. M. Moroz, Nonlinear dynamics in Langmuir circulations and in thermosolutal convection, *J. Fluid Mech.*, *198*, 471–511, 1989.

Lele, S. K., Some problems in hydrodynamic stability arising in geophysical fluid dynamics, Ph.D. thesis, Cornell Univ.,Ithaca, N.Y., 1985.

Press, W. H., B. P. Flannery, S. A. Teukolsky, and W. T. Vetterling, *Numerical Recipes: The Art of Scientific Computing*, Cambridge University Press, NewYork, 1986.

Tandon, A., Direct numerical simulations and hydrodynamic stability problems in the upper oceanic mixed layer, Ph.D. thesis, Cornell Univ., Ithaca, N.Y., 1992.

Thorpe, S. A., The breakup of Langmuir circulation and the instability of an array of vortices, *J. Phys. Oceanogr.*, *22*, 350–360, 1992.

Weller, R. A., and J. F. Price, Langmuir circulation within the oceanic mixed layer, *Deep Sea Res.*, *35*, 711–747, 1988.

S. Leibovich, Sibley School of Mechanical and Aerospace Engineering, Upson Hall, Cornell University, Ithaca, NY 14853-7501.

A. Tandon, Centre for Earth and Ocean Research, P. O. Box 3055, Victoria, B.C., Canada V8W 3P6.

(Received October 30, 1992;
accepted February 10, 1993.)